The influence of object-colour knowledge on emerging object representations in the brain

Abbreviated Title: Colour knowledge and object representations

Lina Teichmann*[1,2], Genevieve L. Quek[5], Amanda K. Robinson[1,2,3], Tijl Grootswagers[1,2,3], Thomas A. Carlson[2,3], Anina N. Rich[1,2,4]

1| Perception in Action Research Centre & Department of Cognitive Science, Macquarie University, Sydney, Australia
2| ARC Centre of Excellence in Cognition & its Disorders, Macquarie University, Sydney, Australia
3| School of Psychology, University of Sydney, Australia
4| Centre for Elite Performance, Training and Expertise, Macquarie University, Sydney, Australia
5| Donders Institute for Brain, Cognition and Behaviour, Radboud University, Nijmegen, The Netherlands

*Corresponding author: lina.teichmann@nih.gov

NUMBER OF WORDS ABSTRACT: 165
NUMBER OF WORDS INTRODUCTION: 644
NUMBER OF WORDS DISCUSSION: 1056
NUMBER OF FIGURES: 7

CONFLICT OF INTERESTS: none

Abstract

The ability to rapidly and accurately recognise complex objects is a crucial function of the human visual system. To recognise an object, we need to bind incoming visual features such as colour and form together into cohesive neural representations and integrate these with our pre-existing knowledge about the world. For some objects, typical colour is a central feature for recognition; for example, a banana is typically yellow. Here, we applied multivariate pattern analysis on time-resolved neuroimaging (magnetoencephalography) data to examine how object-colour knowledge affects emerging object representations over time. Our results from 20 participants (11 female) show that the typicality of object-colour combinations influences object representations, although not at the initial stages of object and colour processing. We find evidence that colour decoding is prolonged for atypical object-colour combinations in comparison to typical object-colour combinations, illustrating the interplay between processing incoming object features and stored object-knowledge. Taken together, these results provide new insights into the integration of incoming visual information with existing conceptual object knowledge.

17

Significance Statement

19 To recognise objects, we have to be able to bind object features such as colour and shape

20 into one coherent representation and compare it to stored object knowledge. The

21 magnetoencephalography data presented here provide novel insights about the integration of

22 incoming visual information with our knowledge about the world. Using colour as a model to

23 understand the interaction between seeing and knowing, we show that there is a unique

24 pattern of brain activity for congruently coloured objects (e.g., a yellow banana) relative to

25 incongruently coloured objects (e.g., a red banana). This effect of object-colour knowledge

26 only occurs after single object features are processed, demonstrating that conceptual

27 knowledge is accessed relatively late in the visual processing hierarchy.

Introduction

Successful object recognition depends critically on comparing incoming perceptual information with existing internal representations (Albright, 2012; Clarke & Tyler, 2015). A central feature of many objects is colour, which can be a highly informative cue in visual object processing (Rosenthal et al., 2018). Although we know a lot about colour perception itself, comparatively less is known about how object-colour knowledge interacts with colour perception and object processing. Here, we measure brain activity with magnetoencephalography (MEG) and apply multivariate pattern analyses (MVPA) to test how stored object-colour knowledge influences emerging object representations over time.

Colour plays a critical role in visual processing by facilitating scene and object recognition (Gegenfurtner & Rieger, 2000; Tanaka et al., 2001), and by giving an indication of whether an object is relevant for behaviour (Conway, 2018; Rosenthal et al., 2018). Objects that include colour as a strong defining feature have been shown to activate representations of associated colours (Bannert & Bartels, 2013; Hansen et al., 2006; Olkkonen et al., 2008; Teichmann et al., 2019; Vandenbroucke et al., 2014; Witzel et al., 2011), leading to slower recognition when there is conflicting colour information (e.g., a red banana; Nagai & Yokosawa, 2003; Tanaka & Presnell, 1999; for a meta-analysis, see Bramão, Reis, Petersson, & Faísca, 2011). Neuroimaging studies on humans and non-human primates have shown that there are several colour-selective regions along the visual ventral pathway (Lafer-Sousa et al., 2016; Lafer-Sousa & Conway, 2013; Seymour et al., 2010, 2015; Zeki & Marini, 1998). While the more posterior colour-selective regions do not show a shape bias, the anterior colour-selective regions do (Lafer-Sousa et al., 2016), supporting suggestions that colour knowledge is represented in regions associated with higher-level visual processing (Simmons et al., 2007; Tanaka et al., 2001). A candidate region for the integration of stored knowledge and incoming visual information is the anterior temporal lobe (ATL; Chiou et al., 2014; Papinutto et al., 2016; Patterson et al., 2007). In one study (Coutanche & Thompson-Schill, 2014), for example, brain activation patterns evoked by recalling a known object's colour and its shape could be distinguished in a subset of brain areas that have been associated with perceiving those features, namely V4 and lateral occipital cortex, respectively. In contrast, recalling an object's particular conjunction of colour *and* shape, could only be distinguished in the ATL, suggesting that the ATL processes conceptual object representations.

Time-resolved data measured with electroencephalography (EEG) or MEG can give an understanding of how conceptual-level processing interacts dynamically with perception.

3

63   Previous EEG studies have examined the temporal dynamics of object-colour knowledge as

64   an index of the integration of incoming visual information and prior knowledge (Lloyd-Jones et

65   al., 2012; Lu et al., 2010; Proverbio et al., 2004). For example, Lloyd-Jones et al. (2012)

66   showed that shape information modulates neural responses at ~170ms (component N1), the

67   combination of shape and colour affected the signal at 225ms (component P2), and the

68   typicality of object-colour pairing modulated components approximately 225 and 350ms after

69   stimulus onset (P2 and P3). These findings suggest that the initial stages of object recognition

70   may be driven by shape, with the interactions with object-colour knowledge coming into play

71   at a much later stage, perhaps as late as during response selection.

72

73   Using multivariate methods for time-resolved neuroimaging data, we can move beyond

74   averaged measures (i.e., components) to infer what type of information is contained in the

75   neural signal on a trial-to-trial basis. In the present study, we used MVPA to determine the

76   timepoint at which neural activity evoked by congruently (e.g., yellow banana) and

77   incongruently (e.g., red banana) coloured objects differs, which indicates when stored

78   knowledge is integrated with incoming visual information. Furthermore, we examined whether

79   existing knowledge about an object's colour influences perceptual processing of surface

80   colour and object identity. Overall, using colour as a model, our findings elucidate the

81   timecourse of interactions between incoming visual information and prior knowledge in the

82   brain.

83

84

85   # Materials and Methods

86   **Participants**

87   20 healthy volunteers (11 female, mean age = 28.9 years, SD = 6.9 years, 1 left-handed)

88   participated in the study. All participants reported accurate colour-vision and had normal or

89   corrected-to-normal visual acuity. Participants gave informed consent before the experiment

90   started and were financially compensated. The study was approved by the Macquarie

91   University Human Research Ethics Committee.

92

93   **Stimuli**

94   We identified five real world objects that previous studies have shown to be strongly

95   associated with each of four different colours (red, green, orange and yellow; see Figure 1)

96   (Bannert & Bartels, 2013; Joseph, 1997; Lloyd-Jones et al., 2012; Naor-Raz et al., 2003;

97   Tanaka & Presnell, 1999; Therriault et al., 2009). Each colour category had one manmade

98   object (e.g., fire hydrant), one living object (e.g., ladybird), and three fruits or vegetables (e.g.,

99   strawberry, tomato, cherry). We sourced two exemplar images for each object class, resulting

100   in 10 images for each colour, 40 individual images in total. We then created incongruently

101   coloured objects by swapping the colours (e.g., yellow strawberry, red banana). For both

102   congruent and incongruent stimuli, we did not use the native colours from the images

103   themselves, but instead overlayed pre-specified hues on desaturated (greyscale) images that

104   were equated for luminance using the SHINE toolbox (Willenbockel et al., 2010). A greyscale

105   image overlayed with its canonically associated colour (e.g., yellow hue applied to greyscale

106   banana) resulted in a congruent object; a greyscale image overlayed with a colour different

107   from its canonically associated colour (e.g., red hue applied to greyscale banana) resulted in

108   an incongruent object. Every congruent object exemplar had a single colour-matched

109   incongruent partner. For example, we used a specific shade of red and added it to the grey-

110   scale images of the strawberry to make the congruent strawberry and overlayed it onto the

111   lemon to make the incongruent lemon. We then took a specific shade of yellow and overlayed

112   it on the lemons to make the congruent lemon exemplar, and onto the strawberry to make the

113   incongruent strawberry exemplar. That means, overall, we have the identical objects and

114   colours in the congruent and the incongruent condition, a factor that is crucial to ensure our

115   results cannot be explained by features other than colour congruency. The only difference

116   between these key conditions is that the colour-object combination is either typical (congruent)

117   or atypical (incongruent).

118

119   This procedure resulted in 40 congruent objects (10 of each colour), and 40 incongruent

120   objects (10 of each colour, Figure 1). We added two additional stimulus types to this set: the

121   full set of 40 greyscale images, and a set of 10 different angular abstract shapes, coloured in

122   each of the four hues for a set of 40 (see Figure 1). As is clear in Figure 1, the colours of the

123   abstract shapes appeared brighter than the colours of the objects, this is because the latter

124   were made by overlaying hue on greyscale, whereas the shapes were simply coloured. As

125   our principle goal was to ensure that the congruent objects appeared to have their typical

126   colouring, we did not match the overall luminance of the coloured stimuli. For example, if we

127   equated the red of a cherry with the yellow of a lemon, neither object would look typically

128   coloured. Thus, each specific colour pair is not equated for luminance; however, we have the

129   same colours across different conditions. The mean chromaticity values and mean lightness

130   for each object are shown in in the Supplementary Information (Figure SI1).

131

132   All stimuli were presented at a distance of 114cm. To add visual variability, which reduces the

133   low-level featural overlap between the images, we varied the image size from trial to trial by 2

134   degrees of visual angle. The range of visual angles was therefore between ∼4.3 – 6.3 degrees.
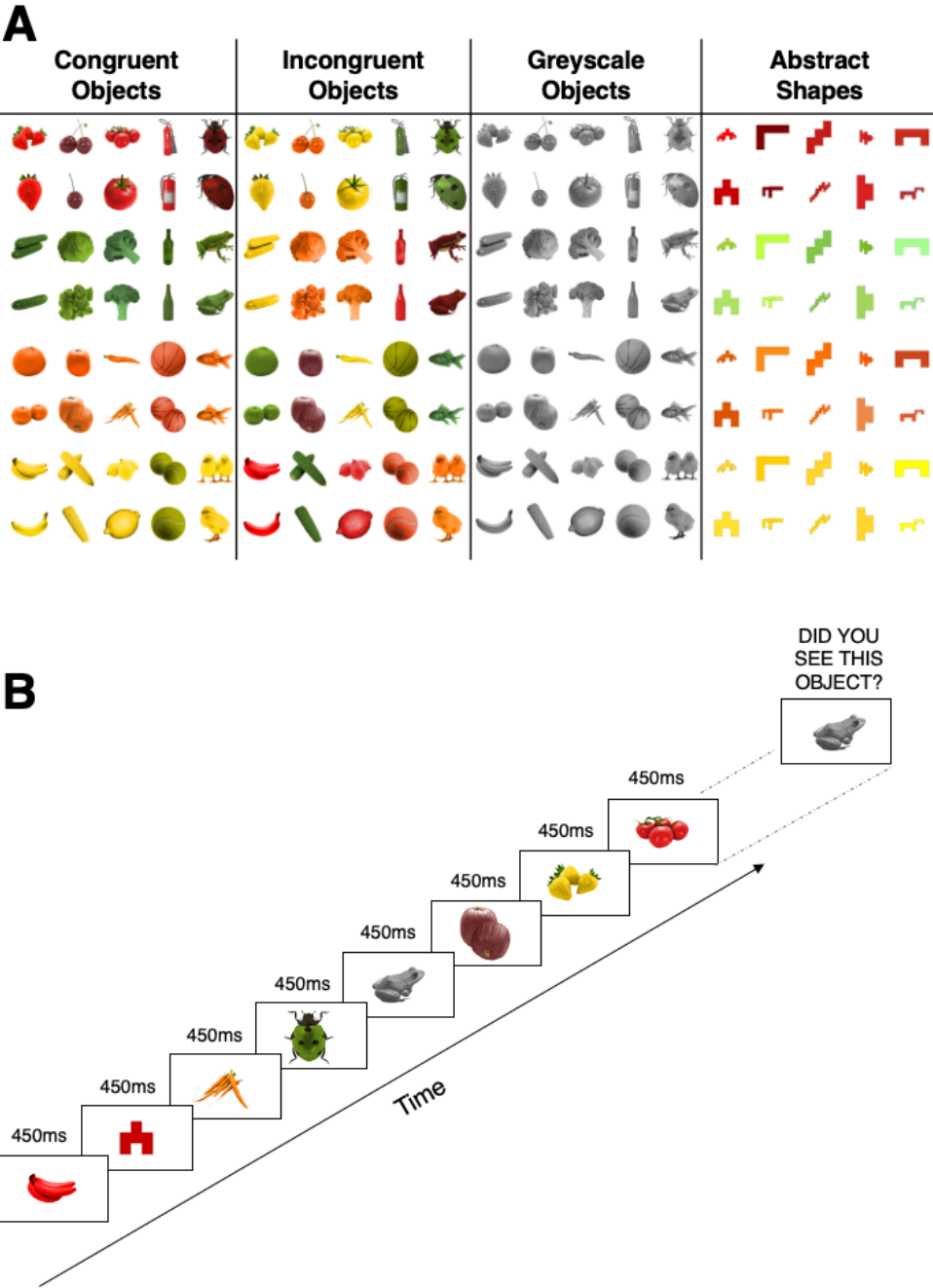
135

136   **Experimental Design and Statistical Analysis**

137   *Experimental tasks*

138   In the main task (Figure 1B), participants completed eight blocks of 800 stimulus presentations

139   each. Each individual stimulus appeared 40 times over the course of the experiment. Each

140   stimulus was presented centrally for 450ms with a black fixation dot on top of it. To keep

141   participants attentive, after every 80 stimulus presentations, a target image was presented

142   until a response was given indicating whether this stimulus had appeared in the last 80

143   stimulus presentations or not (50% present vs absent). The different conditions (congruent,

144   incongruent, grey-scale, abstract shape) were randomly intermingled throughout each block,

145   and the target was randomly selected each time. On average, participants performed with

146   90% (SD=5.4%) accuracy.

147

148   After completing the main blocks, we collected behavioural object-naming data to test for a

149   behavioural congruency effect with our stimuli. On the screen, participants saw each of the

150   objects again (congruent, incongruent or greyscale) in a random order and were asked to

151   name the objects as quickly as possible. As soon as voice onset was detected, the stimulus

152   disappeared. We marked stimulus-presentation times with a photodiode and recorded voice-

153   onset with a microphone. Seventeen participants completed three blocks of this reaction time

154   task, one participant completed two blocks, and for two participants we could not record any

155   reaction times. Each block contained all congruent, incongruent and grey-scale objects

156   presented once.

157

158   Naming reaction times were defined as the difference between stimulus-onset and voice-

159   onset. Trials containing naming errors and microphone errors were not analysed. We

160   calculated the median naming time for each exemplar for each person and then averaged the

161   naming times for each of the congruent, incongruent and greyscale conditions.

162

Figure 1. (A) shows all stimuli used in this experiment. The same objects were used in the congruent, incongruent, and greyscale conditions. There were two exemplars of each objects. Colours in the congruent and incongruent condition were matched. The abstract shapes were identical across colour categories. (B) shows an example sequence of the main task. Participants viewed each object for 450ms. After each sequence, one object was displayed and participants had to indicate whether they had seen this object in the previous sequence or not.

7

174 *MEG data acquisition*

175 While participants completed the main task of the experiment, neuromagnetic recordings were

176 conducted with a whole-head axial gradiometer MEG (KIT, Kanazawa, Japan), containing 160

177 axial gradiometers. We recorded the MEG signal with a 1000Hz frequency. An online low-

178 pass filter of 200Hz and a high-pass filter of 0.03Hz were used. All stimuli were projected on

179 a translucent screen mounted on the ceiling of the magnetically shielded room. Stimuli were

180 presented using MATLAB with Psychtoolbox extension (Brainard, 1997; Brainard & Pelli,

181 1997; Kleiner et al., 2007). Parallel port triggers and the signal of a photodiode were used to

182 mark the beginning and end of each trial. A Bimanual 4-Button Fiber Optic Response Pad

183 (Current Designs, Philadelphia, USA) was used to record the responses.

184

185 Before entering the magnetically shielded room for MEG recordings, an elastic cap with five

186 marker coils was placed on the participant's head. We recorded head shape with a Polhemus

187 Fastrak digitiser pen (Colchester, USA) and used the marker coils to measure the head

188 position within the magnetically shielded room at the start of the experiment, halfway through

189 and at the end.

190

191 *MEG data analysis: Preprocessing*

192 FieldTrip (Oostenveld et al., 2011) was used to preprocess the MEG data. The data were

193 downsampled to 200Hz and then epoched from -100 to 500ms relative to stimulus onset. We

194 did not conduct any further preprocessing steps (filtering, channel selection, trial-averaging

195 etc.) to keep the data in its rawest possible form.

196

197 *MEG data analysis: Decoding Analyses*

198 For all our decoding analyses, patterns of brain activity were extracted across MEG sensors

199 at every timepoint, for each participant separately. We used a regularised linear discriminant

200 analysis (LDA) classifier which was trained to distinguish the conditions of interest. We then

201 used independent test data to assess whether the classifier could predict the condition above

202 chance in the new data. We conducted training and testing at every timepoint and tested for

203 significance using random-effects Monte Carlo cluster (TFCE; Smith & Nichols, 2009)

204 statistics, corrected for multiple comparisons using the max statistic across time points (Maris

205 & Oostenveld, 2007). Note that our aim was not to achieve the highest possible decoding

206 accuracy, but rather to test whether the classifier could predict the conditions above chance

207 at any of the timepoints (i.e., "classification for interpretation", Hebart & Baker, 2017).

208 Therefore, we followed a minimal preprocessing pipeline and performed our analyses on a

209   single-trial basis. Classification accuracy above chance indicates that the MEG data contains

210   information that is different for the categories. We used the CoSMoMVPA toolbox (Oosterhof

211   et al., 2016) to conduct all our analyses.

212

213   We ran several decoding analyses which can be divided in three broad themes. First, we

214   tested when we can differentiate between trials where congruently and incongruently coloured

215   objects were presented. This gives us an indication of the timecourse of the integration of

216   visual object representations and stored conceptual knowledge. Second, we examined single

217   feature processing focusing on colour processing and how the typicality of object-colour

218   combinations influences colour processing over time. Third, we looked at another single

219   feature, shape, and tested whether object-colour combinations influence shape processing

220   over time.

221

222   For the congruency analysis (Figure 2A), we tested whether activation patterns evoked by

223   congruently coloured objects (e.g., red strawberry) differ from activation patterns evoked by

224   incongruently coloured objects (e.g., yellow strawberry). Any differential response that

225   depends on whether a colour is typical or atypical for an object (a congruency effect) requires

226   the perceived shape and colour to be bound and compared to a conceptual object

227   representation activated from memory. We trained the classifier on all congruent and

228   incongruent trials *except* for trials corresponding to one pair of matched exemplars (e.g., all

229   instances of congruent and incongruent strawberries and congruent and incongruent

230   bananas). We then tested the classifier using only the left-out exemplar pairs. We repeated

231   this process until each matched exemplar pair had been left out (i.e., used as test data) once.

232   Leaving an exemplar pair out ensures that there are identical objects and colours for both

233   classes (congruent and incongruent) in both the training and the testing set, and that the

234   stimuli of the test set have different shape characteristics than any of the training objects. As

235   such, the only distinguishing feature between the conditions is the *conjunction* of shape and

236   colour features, which defines congruency. This allows us to compare directly whether (and

237   at which timepoint) stored object representations interacts with incoming object-colour

238   information.

239

240   Next, we focused on the timecourse of colour processing. First, we examined the timecourse

241   of colour processing independent of congruency (Figure 3A). For this analysis, we trained the

242   classifier on distinguishing between the four different colour categories of the abstract shapes

243   and tested its performance on an independent set of abstract shape trials. We always left one

9

244   block out for the cross-validation (8-folds). The results of this analysis give an indication about

245   the emergence of when the representations differ between different surface colours, but as

246   we did not control the colours to be equal in luminance or have the same hue difference

247   between each pair, this is not a pure chromatic measure. We did not control luminance

248   because we used these colours to create our coloured objects, which needed to look as

249   realistic as possible. Thus, the colour decoding analysis includes large and small differences

250   in hue *and in luminance* between the categories. To look at the differences between each

251   colour pair, we also present confusion matrices showing the frequencies of the predicted

252   colour categories at peak decoding.

253

254   Our second colour processing analysis was to examine whether the conjunction of object and

255   colour influenced colour processing (Figure 4A). Perceiving a strongly associated object in the

256   context of viewing a certain colour might lead to a more stable representation of that colour in

257   the MEG signal. For example, if we see a yellow banana, the banana shape may facilitate a

258   representation of the colour yellow earlier than if we see a yellow strawberry. To assess this

259   possibility, we trained the classifier to distinguish between the surface colours of the abstract

260   shapes (i.e., red, orange, yellow, green; chance: 25%). We then tested how well the classifier

261   could predict the colour of the congruent and incongruent objects. Training the classifier on

262   the same abstract shapes across colour categories makes it impossible that a certain shape-

263   colour combination drives an effect, as the only distinguishing feature between the abstract

264   shapes is colour. This analysis allows us to compare whether the typicality of colour-form

265   combinations has an effect on colour processing.

266

267   In our final set of analyses, we examined the timecourse of shape processing. First, to assess

268   the timecourse of shape processing independent of congruency, we trained a classifier to

269   distinguish the five different abstract shapes in a pairwise fashion (Figure 5A). We always

270   used one independent block of abstract shape trials to test the classifier performance (8-fold

271   cross-validation). The results of this analysis indicate when information about different shapes

272   are is present in the neural signal, independent of other object features (e.g., colour) or

273   congruency. Second, we tested whether the conjunction of object and colour has an effect on

274   object decoding (Figure 6A). If object-colour influences early perceptual processes, we might

275   see a facilitation for decoding objects when they are coloured congruently or interference

276   when the objects are coloured incongruently. We used the greyscale object trials to train the

277   classifier to distinguish between all of the objects. The stimulus set contained two exemplars

278   of each item (e.g., strawberry 1 and strawberry 2). We used different exemplars for the training

279   and testing set to minimise the effects of low-level visual features, however, given that there

280   are major differences in object shapes and edges, we can still expect to see strong differences

281   between the objects. The classifier was trained on one exemplar of all of the greyscale trials.

282   We then tested the classifier's performance on the congruent and incongruent object trials

283   using the exemplars the classifier did not train on. We then swapped the exemplars used for

284   training and testing set until every combination had been used in the testing set. Essentially,

285   this classifier is trained to predict which object was presented to the participant (e.g., was it a

286   strawberry or a frog?) and we are testing whether there is a difference depending on whether

287   the object is congruently or incongruently coloured.

288

289   *Statistical Inferences*

290   In all our analyses, we used random effects Monte-Carlo cluster statistic using Threshold Free

291   Cluster Enhancement (TFCE, Smith & Nichols, 2009) as implemented in the CoSMoMVPA

292   toolbox to see whether the classifier could predict the condition of interest above chance. The

293   TFCE statistic represents the support from neighbouring time points, thus allowing for

294   detection of sharp peaks and sustained small effects over time. We used a permutation test,

295   swapping labels of complete trials, and re-ran the decoding analysis on the data with the

296   shuffled labels 100 times per participant to create subject-level null-distributions. We then

297   used Monte-Carlo sampling to create a group-level null-distribution consisting of 10,000

298   shuffled label permutations for the time-resolved decoding, and 1000 for the time-

299   generalisation analyses (to reduce computation time). The null distributions were then

300   transformed into TFCE statistics. To correct for multiple comparisons, the *maximum* TFCE

301   values across time in each of the null distributions was selected. We then transformed the true

302   decoding values to TFCE statistics. To assess whether the true TFCE value at each timepoint

303   is significantly above chance, we compared it to the 95th percentile of the corrected null

304   distribution. Selecting the maximum TFCE value provides a conservative threshold for

305   determining whether the observed decoding accuracy is above chance, corrected for multiple

306   comparisons.

307

308   To assess at which timepoint the decoding accuracy peaks, we bootstrapped the participants'

309   decoding accuracies for each analysis 10,000 times and generated 95% confidence intervals

310   for peak decoding. For the analyses in which we are comparing colour and exemplar decoding

311   for congruent and incongruent trials, we also compared the above chance decoding durations.

312   To test for the duration of above chance decoding, we bootstrapped the data (10,000 times)

313   and ran our statistics. At each iteration we then looked for the longest period in which we have

314   above chance decoding in consecutive timepoints. We plotted the bootstrapped decoding

315   durations and calculated medians to compare the distributions for the congruent and the

316   incongruent condition.

317

318

319   **Results**

320   **Behavioural results**

321   We first present the data from our behavioural object-naming task to confirm that our stimuli

322   induce a congruency effect on object naming times. All incorrect responses and microphone

323   errors were excluded from the analysis (on average across participants: 10.1%). We then

324   calculated the median reaction time for naming each stimulus. If a participant named a specific

325   stimulus incorrectly across trials (e.g., incongruently coloured strawberry was always named

326   incorrectly), we removed this stimulus completely to ensure that the reaction times in one

327   condition were not skewed (on average this occurred in 5.4% of cases). Participants were

328   faster to name the congruently coloured (702ms) than incongruently coloured (750ms) objects

329    $(t(17) = 4.06, p < .001; 95\%CI [22.9, 72.7])$. This suggests that the objects we used here do

330   indeed have associations with specific canonical colours, and we replicate that these objects

331   are consistently associated with a particular colour (Bannert & Bartels, 2013; Joseph, 1997;

332   Lloyd-Jones et al., 2012; Naor-Raz et al., 2003; Tanaka & Presnell, 1999; Therriault et al.,

333   2009).

334

335   In the main task, participants were asked to indicate every 80 trials whether they had seen a

336   certain target object or not. The aim of this task was to keep participants motivated and

337   attentive throughout the training session. On average, participants reported whether the

338   targets were present or absent with 90% accuracy (SD = 5%, range: 81.25% - 100%).

339

340   **MEG results**

341   The aim of our decoding analyses was to examine the interaction between object-colour

342   knowledge and object representations. First, we tested for a difference in the brain activation

343   pattern for congruently and incongruently coloured objects. The results show distinct patterns

344   of neural activity for congruent compared to incongruent objects in a cluster of consecutive

345   timepoints stretching from 250 to 325ms after stimulus onset, demonstrating that brain activity

346   is modulated by colour congruency in this time window (Figure 2B). Thus, binding of colour

347   and form must have occurred by ~250ms and stored object-colour knowledge is integrated

348   with incoming information. An exploratory searchlight (Carlson et al., 2019; Collins et al., 2018;

349   Kaiser et al., 2016) across small clusters (9 at a time) of MEG sensors suggests that this effect

350   is driven a range of frontal, temporal and parietal sensor clusters (Figure 2C).
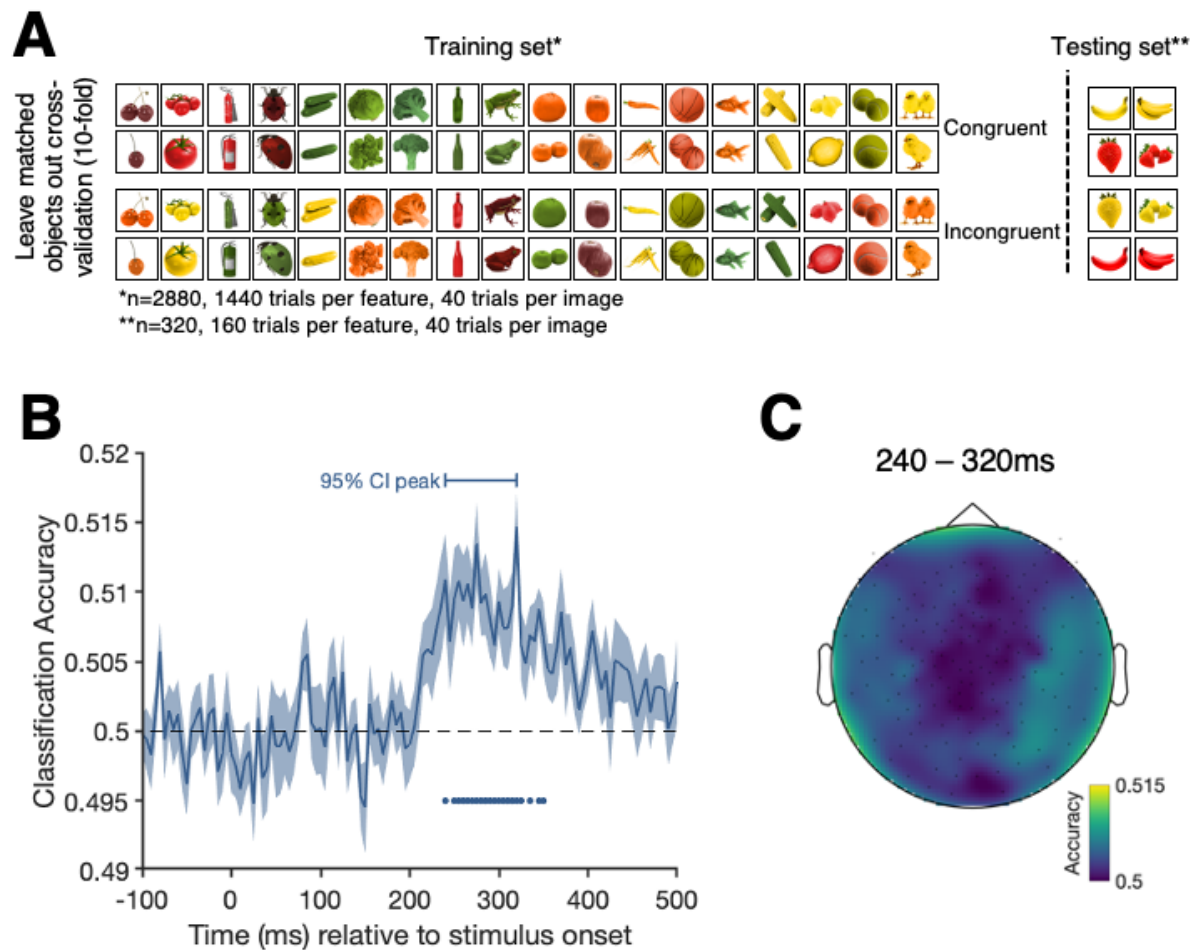
351

352

353   Figure 2. Cross-validation and results of the congruency analysis contrasting trials from the
354   congruent and incongruent conditions. (A) shows the leave-one-matched-exemplar-out cross
355   validation approach for a single fold for the congruency decoding analysis. The classifier was
356   trained on the trials shown on the left and tested on the trials on the right, ensuring that the
357   classifier is not tested on the exemplars that it trained on. This limits the effect features other
358   than congruency can have on classifier performance. (B) shows the classification accuracy
359   over time. Shading represents the standard error across participants. Black dashed line
360   represents chance level (50% - congruent versus incongruent). Filled dots highlight significant
361   timepoints, corrected for multiple comparisons. The horizontal bar above the curve shows the
362   95% confidence interval of the peak. (C) is an exploratory sensor searchlight analysis in which
363   we run the same analysis across small clusters of sensors. The colours highlight the decoding
364   accuracy for each sensor cluster averaged over the 95% confidence interval of the peak
365   timepoints.
366

367   To examine the timecourse of colour processing separately from congruency, we decoded the

368   surface colours of the abstract shapes (Figure 3A). Consistent with earlier results (Teichmann

369   et al., 2019), we found that colour can be decoded above chance from the abstract shape

370   trials in a cluster stretching from 70 to 350ms (Figure 3B). Looking at data from an exploratory

371   sensor searchlight analysis across small clusters of sensors shows that colour information at

372   peak decoding is mainly distinguishable from occipital and parietal sensors. To examine

373   whether all colours could be dissociated equally well, we also looked at confusion matrices

374   displaying how frequently each colour category was predicted for each colour (Figure 3D).

375   The results show that at the decoding peak (140ms), red and green are most easily

376   distinguishable and that the prediction errors are not equally distributed: Red trials are more

377   frequently misclassified as being orange than green or yellow and green trials are more

378   frequently misclassified as being yellow than orange or red. This indicates that colours that

379   are more similar evoke a more similar pattern of activation than colours that are dissimilar

380   (Figure 3E).

381

14

382
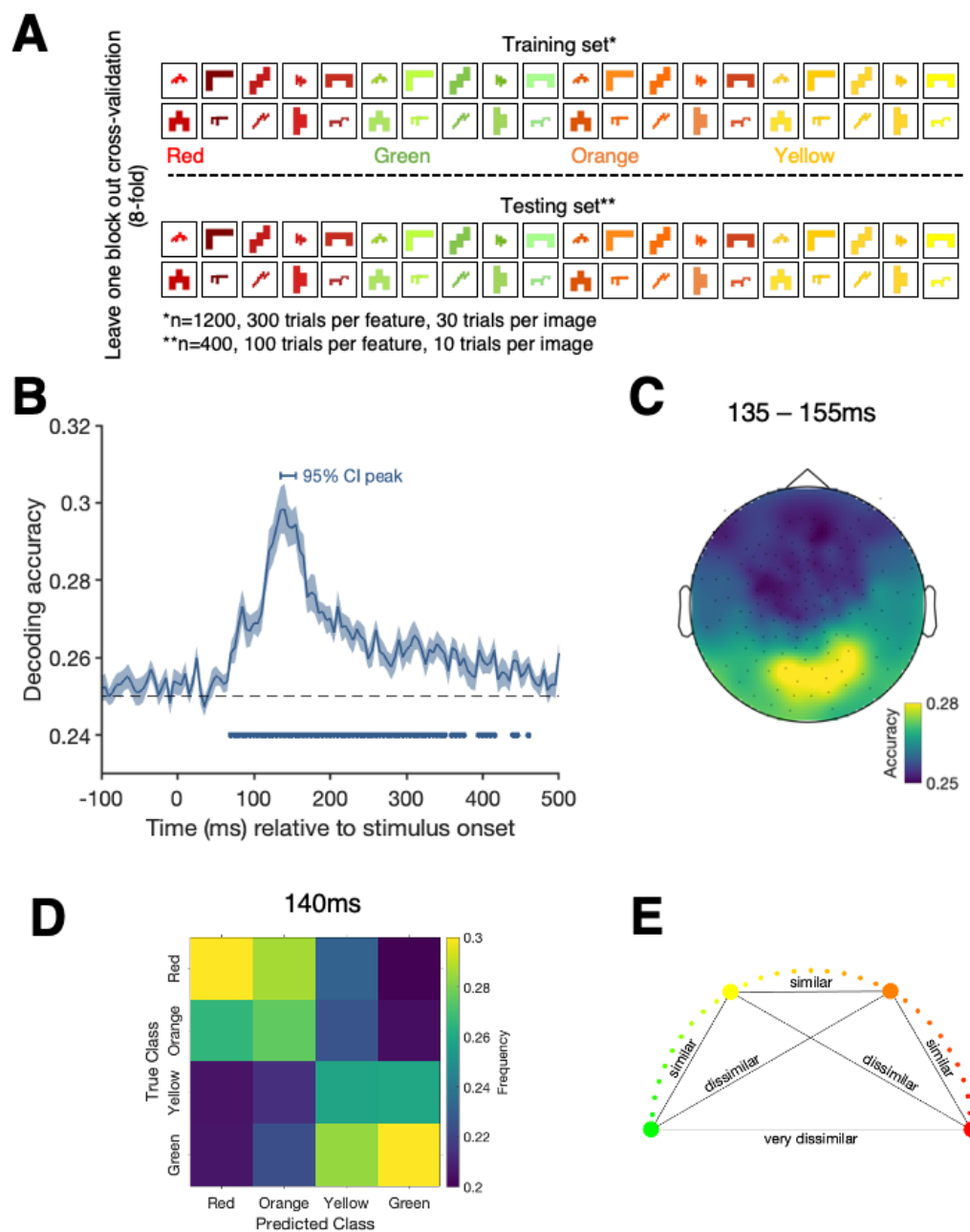
383 Figure 3. (A) depicts the colour decoding analysis when training the classifier to distinguish
384 between the different colour categories of the abstract shapes and testing on a block of
385 independent abstract shape trials. (B) shows the decoding accuracy for the colour decoding
386 analysis over time. Shading represents the standard error across participants. Black dashed
387 line represents chance level (25% - red versus green versus orange versus yellow). Filled dots
388 highlight significant timepoints, corrected for multiple comparisons. The horizontal bar above
389 the curve shows the 95% confidence interval of the peak. (C) shows the results of a
390 exploratory searchlight analysis over small sensor clusters averaged across the timepoints of
391 the 95% confidence interval for peak decoding. Colours indicate the decoding accuracies at
392 each sensor. (D) depicts a confusion matrix for peak decoding (140ms) showing the
393 frequencies at which colour categories were predicted given the true class. (E) shows the
394 similarity of the colour categories which might underlie the results in (D).

395

396

397 To assess whether congruency influences colour processing, we trained a classifier to

398 distinguish between the colours in the abstract shape condition and then tested it on the

399 congruent and incongruent trials separately (Figure 4A). Colour can be successfully classified

400 in a cluster stretching from 75 to 125ms for the congruent condition and in a cluster stretching

401 from 75 to 185ms for the incongruent trials (Figure 4B). These results suggest there may be

402 a difference in the way colour information is processed depending on the congruency of the

403 image, specifically evident in the decoding duration. To test whether there is a true difference

404 in decoding durations, we bootstrapped the data and looked at the longest consecutive streak

405 of above chance decoding. We plotted the distribution and the median of the bootstrapped

406 decoding durations for both congruently and incongruently coloured objects. The data suggest

407 that colour can be decoded for longer in the incongruent compared to congruent condition. To

408 get a complete picture of how these signals evolve over time, we used time-generalisation

409 matrices (Figure 4D and 4E). To create time-generalisation matrices, we trained the classifier

410 on each timepoint of the training dataset and then tested it on all timepoints of the test set.

411 The diagonal of these matrices corresponds to the standard time-resolved decoding results

412 (e.g., training at 100ms and testing at 100ms). A decodable off-the-diagonal effect reflects a

413 temporal asynchrony in information processing in the training and testing set (cf. Carlson et

414 al., 2011; King & Dehaene, 2014). Our data show that colour category was decodable from

415 both conditions early on (~70ms). In the incongruent condition, the activation associated with

416 colour seems to be sustained longer (Figure 4E) than for the congruent condition (Figure 4D),

417 but for both, decoding above chance occurs mainly along the diagonal. This suggests that the

418 initial pattern of activation for colour signals occurs at the same time but that the signals

419 associated with colour are prolonged when object-colour combinations are unusual relative to

420 when they are typical.

421

*n=1600, 400 trials per feature, 40 trials per image

422
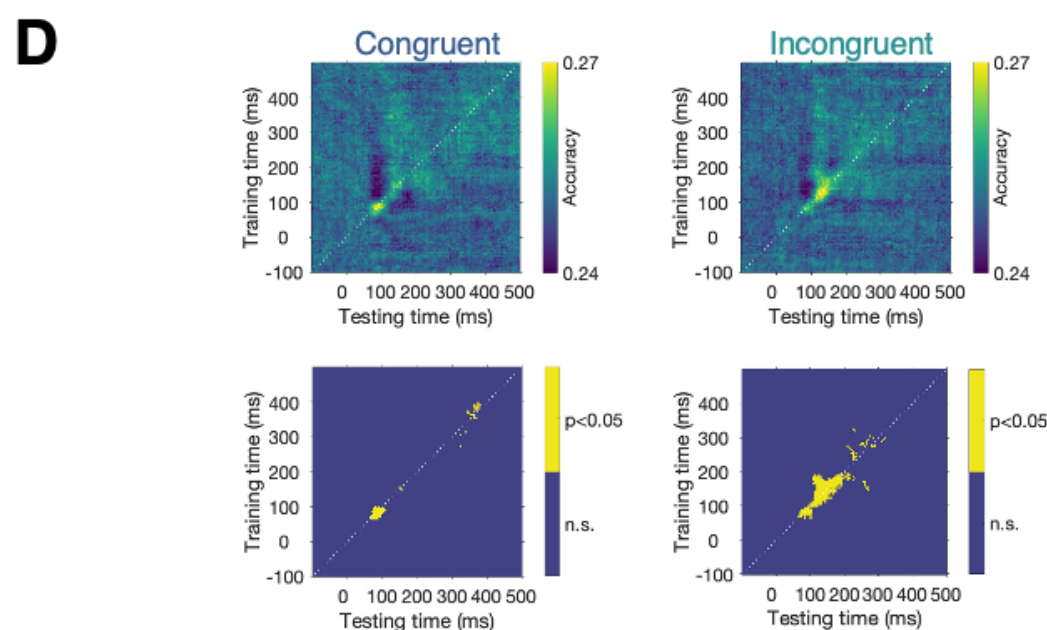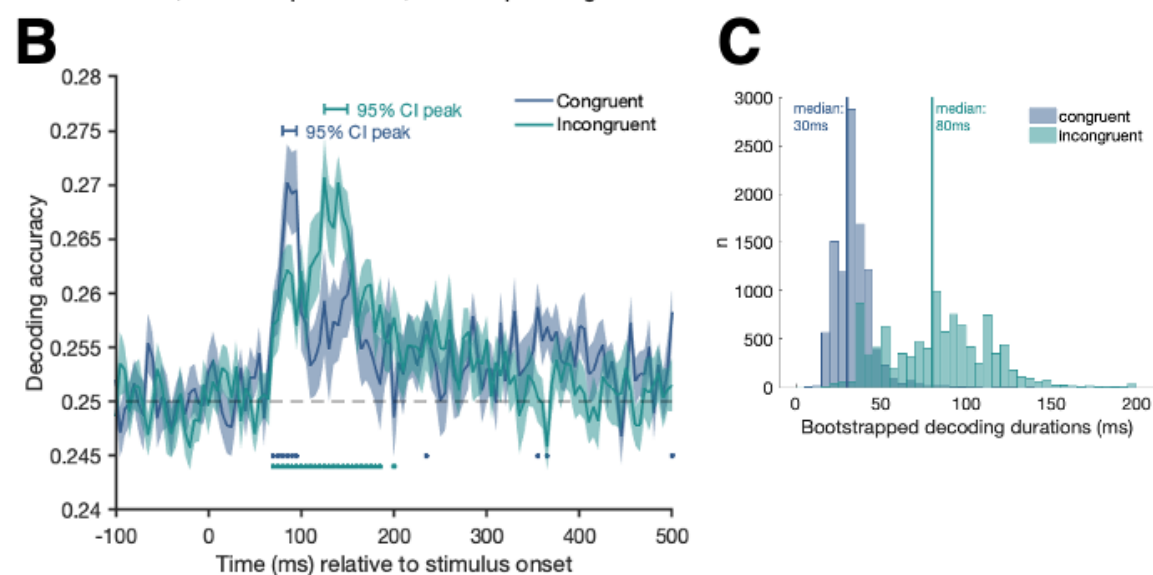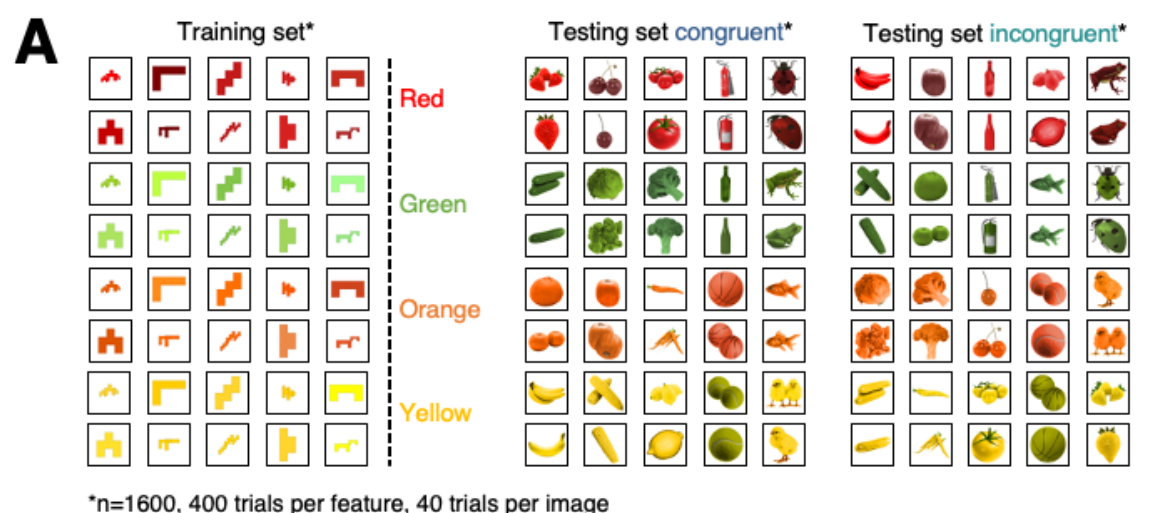
423   Figure 4. Results of the colour decoding analysis for the congruent and incongruent trials.
424   Here, the classifier was trained to distinguish the colour of all abstract shape trials and tested
425   on the congruent and incongruent trials separately (A). (B) shows the classification accuracy
426   over time for the congruent (blue) and incongruent (green) trials. Shading represents the
427   standard error across participants. Black dashed line indicates chance level (25% - red versus
428   green versus orange versus yellow). Blue (congruent) and green (incongruent) dots highlight
429   timepoints at which we can decode the surface colour significantly above chance, corrected
430   for multiple comparisons. (C) shows the bootstrapped decoding duration distributions for the
431   congruent and the incongruent conditions. (D) shows the results of the same analysis across
432   all possible training and testing timepoint combinations. These time-time matrices allow us to
433   examine how the signal for the congruent colours (left) and incongruent colours (right) evolves
434   over time. The top row shows the classification accuracy at every timepoint combination with
435   lighter pixels reflecting higher decoding accuracies. The bottom row shows clusters where
436   decoding is significantly above chance (yellow), corrected for multiple comparisons.

437

438

439   The goal of the third analysis was to examine whether shape representations are affected by

440   colour congruency. It could be the case, for example, that the representation of banana-

441   shapes compared to strawberry-shapes is enhanced when their colours are correct. First, we

442   tested when shape representations can be decoded independent of colour congruency. We

443   trained the classifier to distinguish between the five different abstract shapes in a pairwise

444   fashion and then tested its performance on independent data (Figure 5A). The data show that

445   shape information can be decoded in a cluster stretching from 60 to 500ms (Figure 5B).

446   Running an exploratory searchlight analysis on small clusters of sensors (9 at a time) shows

447   that shape information at peak decoding is mainly driven by occipital sensors.
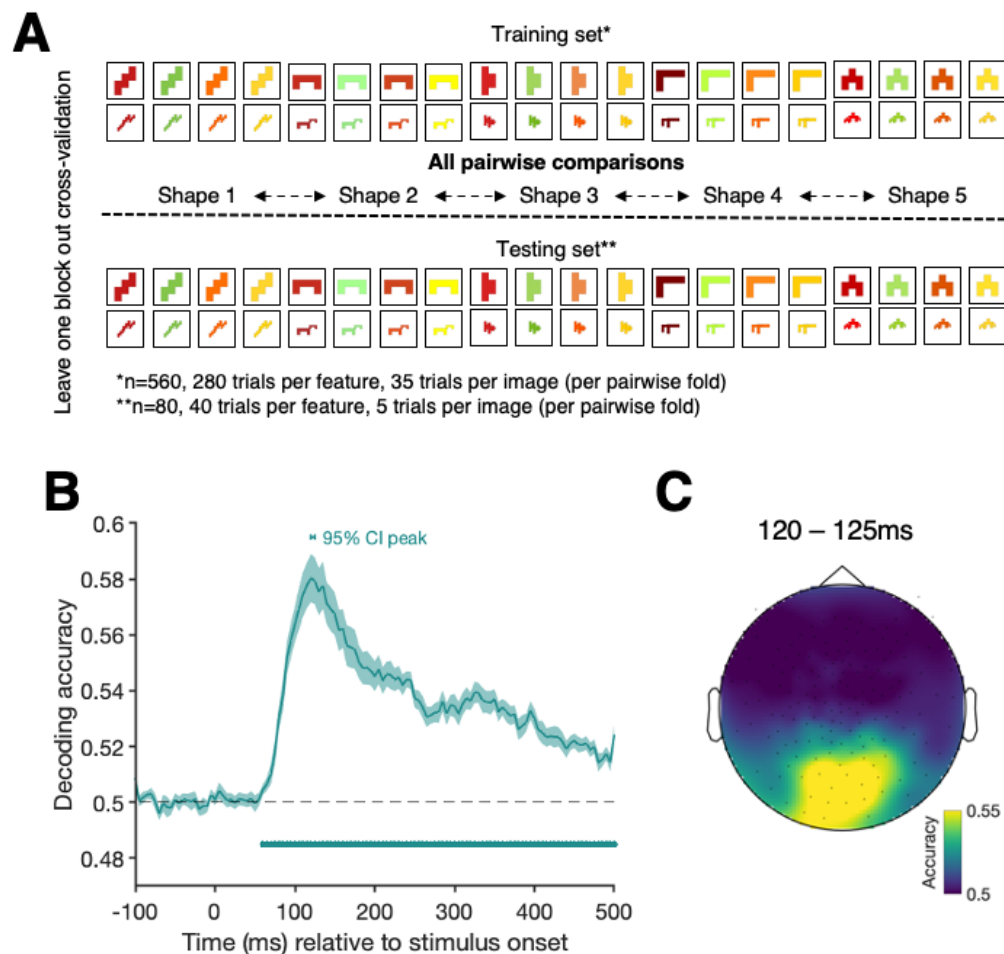
17

Figure 5. (A) depicts the shape decoding analysis when training the classifier to distinguish between the different categories of the abstract shapes and testing on a block of independent abstract shape trials. (B) shows the decoding accuracy for the shape decoding analysis over time. Shading represents the standard error across participants. Black dashed line represents chance level (50% - pairwise comparison of all shapes). Filled dots highlight significant timepoints, corrected for multiple comparisons. The horizontal bar above the curve shows the 95% confidence interval of the peak. (C) shows the results of an exploratory searchlight analysis over small sensor clusters averaged across the timepoints of the 95% confidence interval for peak decoding. Colours indicate the decoding accuracies at each sensor.

To examine whether colour affects object processing, we trained a classifier to distinguish between trials in which the participant saw one of the exemplars of each of the twenty objects in greyscale (e.g., greyscale strawberry 1, greyscale cherry 1, etc.). We then tested at which timepoint the classifier could successfully cross-generalise to the other exemplar of that object in the congruent and incongruent condition separately. If object representations (e.g., banana) are influenced by the typicality of their colours, then cross-generalisation should be different for congruent and incongruent trials. Note that although the exact images are unique, there are shared shape characteristics between exemplars (e.g., the two frog exemplars share

18

468   some shape aspects despite being different postures), which can be expected to drive an

469   effect. The results show the neural data has differential information about the object in a cluster

470   stretching from 65 to 500ms for both the congruent and the incongruent test sets (Figure 5B).

471   These results show that we can decode the object class early on, at a similar time to when we

472   can decode the abstract shape conditions, suggesting that the classifier here is driven strongly

473   by low-level features (like shape), rather than being influenced by colour congruency. The

474   timecourse for congruent and incongruent object decoding is very similar and decoding peaks

475   overlap. Looking at the bootstrapped decoding durations (Figure 5C), we can see that object

476   decoding is above chance for a similar duration in the congruent and the incongruent

477   condition. Thus, our data suggest that there is no effect of colour congruency on object

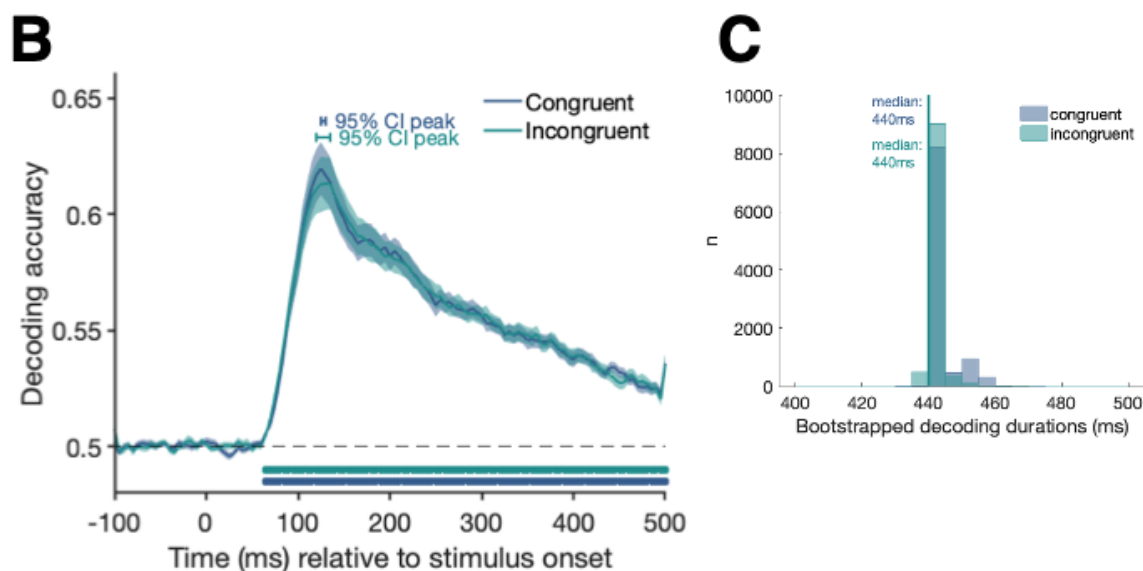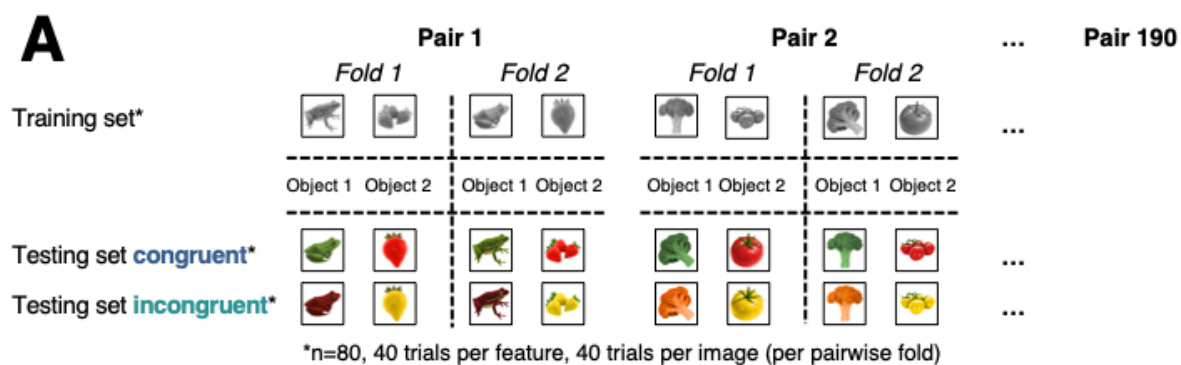478   processing.

479

480

481

482   Figure 6. Results of the object exemplar decoding analysis. The classifier was trained to
483   distinguish between all pairwise object categories in the greyscale object condition. We used
484   one exemplar of each class for the training and the other exemplar for testing the classifier.

19

485 Testing was done for the congruent and incongruent trials separately (A). (B) shows the
486 classification accuracy over time for the object decoding analysis when testing the classifier's
487 performance on congruent (blue) and incongruent (green) trials. Shading represents the
488 standard error across participants. Black dashed line represents chance level (50% - pairwise
489 decoding for all 20 different object categories). Blue (congruent) and green (incongruent) dots
490 highlight significant timepoints (p<0.05), corrected for multiple comparisons. (C) shows the
491 bootstrapped decoding duration distributions for the congruent and the incongruent
492 conditions.
493

494 Overall, the results here show that single features present within the incoming visual stimuli

495 are decodable earlier than the congruency between them, which can be seen as an index for

496 accessing stored conceptual knowledge (Figure 7). When we compare colour and shape

497 decoding for abstract shapes and for congruently and incongruently coloured objects, the

498 decoding onsets are very similar, suggesting the initial processes of single feature

499 processing are not influenced by congruency. However, colour decoding is prolonged for

500 incongruently coloured in comparison to congruently coloured objects suggesting that colour

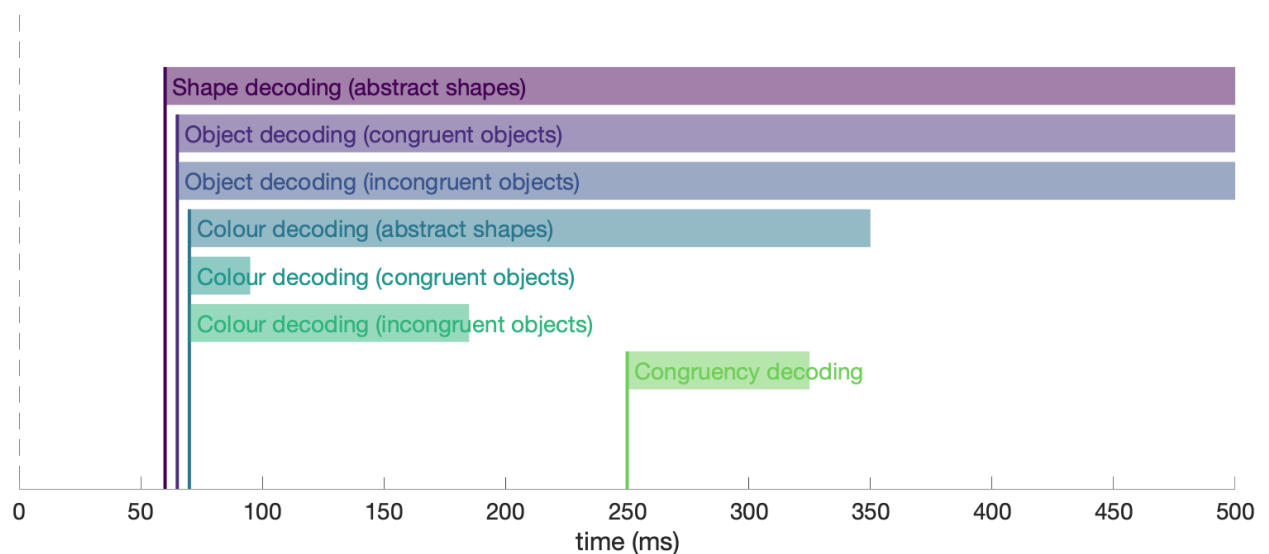501 congruency influences colour processing to some degree.

502
503
504 Figure 7. Overview of the findings. Each coloured bar shows the the onset (x axis) and duration
505 (length of coloured bar) at which feature and conjunction information was contained in the
506 neural signal. The dotted vertical line represents stimulus onset.
507
508
509
510

Discussion

512 A crucial question in object recognition concerns how incoming visual information interacts

513 with stored object concepts to create meaningful vision under varying situations. The aims of

514   the current study were to examine the temporal dynamics of object-colour knowledge and to
515   test whether activating object-colour knowledge influences the early stages of colour and
516   object processing. Our data provide three major insights: First, congruently and incongruently
517   coloured objects evoke a different neural representation after ~250ms suggesting that, by this
518   time, visual object features are bound into a coherent representation and compared to stored
519   object representations. Second, colour can be decoded at a similar latency (~70ms)
520   irrespective of whether participants view coloured abstract shapes, or congruently and
521   incongruently coloured objects. However, the colour signal is prolonged when viewing
522   incongruently coloured objects compared to congruent ones. Third, we do not find an influence
523   of colour congruency on object processing, which may suggest that behavioural congruency
524   effects are due to conflict at a later stage in processing.

525

526   Colour congruency can act as an index to assess when prior knowledge is integrated with
527   bound object features. When comparing brain activation patterns of the same objects
528   presented in different colours, there was a decodable difference between congruent and
529   incongruent conditions from ~250ms onwards suggesting a stored object representation that
530   contains information about the typical colour of an object must have been activated by this
531   stage. Prior to this time, the signal is primarily driven by processing of early perceptual features
532   such as colour and shape, which were matched for the congruent and incongruent conditions
533   (same objects, same colours, only the combination of colour and shape differed). Although
534   from our data we cannot draw direct conclusions about which brain areas are involved in the
535   integration of incoming visual information and stored object knowledge, our congruency
536   analysis adds to the fMRI literature by showing the relative timecourse at which a meaningful
537   object representation emerges. Activating object-colour knowledge from memory has been
538   shown to involve the ATL (e.g., Coutanche & Thompson-Schill, 2014) and there is evidence
539   that object-colour congruency coding occurs in perirhinal cortex (Price et al., 2017). Further
540   support on the involvement of the ATL in the integration of incoming sensory information and
541   stored representations comes from work on patients with semantic dementia (e.g., Bozeat et
542   al., 2002) and studies on healthy participants using TMS (e.g., Chiou et al., 2014). Higher level
543   brain areas in the temporal lobe have also been shown to be part of neuronal circuits involved
544   in implicit imagery, supporting visual perception by augmenting incoming information with
545   stored conceptual knowledge (e.g., Albright, 2012; Miyashita, 2004). The latency of
546   congruency decoding here may thus reflect the time it takes to compare visual object
547   representations with conceptual templates in higher-level brain areas such as the ATL, or the

548   time it takes for feedback or error signals about colour congruency to arrive back in early visual

549   areas.

550

551   Our results also show that colour congruency has an effect on colour processing. We found

552   colour decoding onset at a similar time (~70ms) for abstract shapes and congruently and

553   incongruently coloured objects. This indicates that colour signals are activated initially

554   independently of object shape, consistent with previous work showing that single features are

555   processed first and that the conjunction of colour and shape occurs at a later stage (e.g.,

556   Seymour et al., 2015). However, we also found differences between colour processing in

557   congruent and incongruent conditions: The duration of the colour signal was longer and

558   peaked later in the incongruent relative to the congruent condition, suggesting that congruency

559   influences the timecourse of colour processing to some degree. Our time-generalisation

560   analysis (Figure 4D) supports this by showing that there is a different dynamic for congruent

561   and incongruent trials. One possible explanation for this finding is that unusual feature pairings

562   (e.g., shape and colour or texture and colour) might lead to local feedback signals that prolong

563   colour processing. Alternatively, consistent with the memory colour literature (e.g., Hansen et

564   al., 2006; Olkkonen et al., 2008; Witzel et al., 2011), it is possible that typical colours are co-

565   activated along with other low-level features. For incongruent trials, this would then lead to

566   two potential colours needing to be distinguished, extending the timeframe for processing and

567   delaying the peak activation for the surface colour of the object.

568

569   The timecourse of exemplar decoding we present is consistent with previous studies on object

570   recognition. Here, we found that exemplar identity could be decoded at ~65ms. Similar

571   latencies have been found in other M/EEG decoding studies (Carlson et al., 2013; Cichy et

572   al., 2014; Contini et al., 2017; Grootswagers et al., 2019; Isik et al., 2013) and single unit

573   recordings (e.g., Hung, Kreiman, Poggio, & DiCarlo, 2005). Behavioural data, including the

574   reaction times collected from our participants, show that colour influences object identification

575   speed (e.g., Bramão, Faísca, Petersson, & Reis, 2010). The neural data, however, did not

576   show an effect of object colour on the classifier's performance when distinguishing the neural

577   activation patterns evoked by different object exemplars. For example, the brain activation

578   pattern in response to a strawberry could be differentiated from the pattern evoked by a lemon,

579   regardless of the congruency of their colours. This finding is consistent with previous results

580   (Proverbio et al., 2004) but might seem puzzling because colour congruency has been shown

581   to have a strong effect on object naming (e.g., Chiou et al., 2014; Nagai & Yokosawa, 2003;

582   Tanaka & Presnell, 1999). One plausible possibility is that the source of behavioural

583   congruency effects may be at the stage of response selection, which would not show up in

584   these early neural signals. More evidence is needed, but there is no evidence in the current

585   data to suggest colour congruency influences early stages of object processing.

586

587   Our data demonstrate that object representations are influenced by object-colour knowledge

588   but not at the initial stages of visual processes. Consistent with a traditional hierarchical view,

589   we show that visual object features are processed before the features are bound into a

590   coherent object that can be compared with existing, conceptual object representations.

591   However, our data also suggest that the temporal dynamics of colour processing are

592   influenced by the typicality of object-colour pairings. Building on the extensive literature on

593   visual perception, these results provide a timecourse for the integration of incoming visual

594   information with stored knowledge, a process that is critical for interpreting the visual world

595   around us.

References

Albright, T. D. (2012). On the perception of probable things: Neural substrates of associative memory, imagery, and perception. *Neuron*, *74*(2), 227–245.

Bannert, M. M., & Bartels, A. (2013). Decoding the yellow of a gray banana. *Current Biology*, *23*(22), 2268–2272.

Bozeat, S., Lambon Ralph, M. A., Patterson, K., & Hodges, J. R. (2002). When objects lose their meaning: What happens to their use? *Cognitive, Affective, & Behavioral Neuroscience*, *2*(3), 236–251.

Brainard, D. H. (1997). The psychophysics toolbox. *Spatial Vision*, *10*, 433–436.

Brainard, D. H., & Pelli, D. G. (1997). The psychophysics toolbox. *Spatial Vision*, *10*, 433–436.

Bramão, I., Faísca, L., Petersson, K. M., & Reis, A. (2010). The influence of surface color information and color knowledge information in object recognition. *The American Journal of Psychology*, *123*(4), 437–446.

Carlson, T. A., Grootswagers, T., & Robinson, A. K. (2019). An introduction to time-resolved decoding analysis for M/EEG. *ArXiv Preprint ArXiv:1905.04820*.

Carlson, T. A., Hogendoorn, H., Kanai, R., Mesik, J., & Turret, J. (2011). High temporal resolution decoding of object position and category. *Journal of Vision*, *11*(10), 9–9.

Carlson, T. A., Tovar, D. A., Alink, A., & Kriegeskorte, N. (2013). Representational dynamics of object vision: The first 1000 ms. *Journal of Vision*, *13*(10), 1–1.

Chiou, R., Sowman, P. F., Etchell, A. C., & Rich, A. N. (2014). A conceptual lemon: Theta burst stimulation to the left anterior temporal lobe untangles object

representation and its canonical color. *Journal of Cognitive Neuroscience*, *26*(5), 1066–1074.

Cichy, R. M., Pantazis, D., & Oliva, A. (2014). Resolving human object recognition in space and time. *Nature Neuroscience*, *17*(3), 455.

Clarke, A., & Tyler, L. K. (2015). Understanding what we see: How we derive meaning from vision. *Trends in Cognitive Sciences*, *19*(11), 677–687.

Collins, E., Robinson, A. K., & Behrmann, M. (2018). Distinct neural processes for the perception of familiar versus unfamiliar faces along the visual hierarchy revealed by EEG. *NeuroImage*, *181*, 120–131.

Contini, E. W., Wardle, S. G., & Carlson, T. A. (2017). Decoding the time-course of object recognition in the human brain: From visual features to categorical decisions. *Neuropsychologia*. https://doi.org/10.1016/j.neuropsychologia.2017.02.013

Conway, B. R. (2018). The organization and operation of inferior temporal cortex. *Annual Review of Vision Science*, *4*, 381–402.

Coutanche, M. N., & Thompson-Schill, S. L. (2014). Creating concepts from converging features in human cortex. *Cerebral Cortex*, *25*(9), 2584–2593.

Gegenfurtner, K. R., & Rieger, J. (2000). Sensory and cognitive contributions of color to the recognition of natural scenes. *Current Biology*, *10*(13), 805–808. https://doi.org/10.1016/S0960-9822(00)00563-7

Grootswagers, T., Robinson, A. K., & Carlson, T. A. (2019). The representational dynamics of visual objects in rapid serial visual processing streams. *NeuroImage*, *188*, 668–679.

Hansen, T., Olkkonen, M., Walter, S., & Gegenfurtner, K. R. (2006). Memory modulates color appearance. *Nature Neuroscience*, *9*(11), 1367.

Hebart, M. N., & Baker, C. I. (2018). Deconstructing multivariate decoding for the study of brain function. *Neuroimage*, *180*, 4–18.

Hung, C. P., Kreiman, G., Poggio, T., & DiCarlo, J. J. (2005). Fast readout of object identity from macaque inferior temporal cortex. *Science*, *310*(5749), 863–866.

Isik, L., Meyers, E. M., Leibo, J. Z., & Poggio, T. (2013). The dynamics of invariant object recognition in the human visual system. *Journal of Neurophysiology*, *111*(1), 91–102. https://doi.org/10.1152/jn.00394.2013

Joseph, J. E. (1997). Color processing in object verification. *Acta Psychologica*, *97*(1), 95–127.

Kaiser, D., Oosterhof, N. N., & Peelen, M. V. (2016). The neural dynamics of attentional selection in natural scenes. *Journal of Neuroscience*, *36*(41), 10522–10528.

King, J. R., & Dehaene, S. (2014). Characterizing the dynamics of mental representations: The temporal generalization method. *Trends in Cognitive Sciences*, *18*(4), 203–210. https://doi.org/10.1016/j.tics.2014.01.002

Kleiner, M., Brainard, D., Pelli, D., Ingling, A., Murray, R., Broussard, C., & others. (2007). What's new in Psychtoolbox-3. *Perception*, *36*(14), 1.

Lafer-Sousa, R., & Conway, B. R. (2013). Parallel, multi-stage processing of colors, faces and shapes in macaque inferior temporal cortex. *Nature Neuroscience*, *16*(12), 1870.

Lafer-Sousa, R., Conway, B. R., & Kanwisher, N. G. (2016). Color-Biased Regions of the Ventral Visual Pathway Lie between Face- and Place-Selective Regions in

Humans, as in Macaques. *Journal of Neuroscience, 36*(5), 1682–1697.

https://doi.org/10.1523/JNEUROSCI.3164-15.2016

Lloyd-Jones, T. J., Roberts, M. V., Leek, E. C., Fouquet, N. C., & Truchanowicz, E.
G. (2012). The time course of activation of object shape and shape+ colour
representations during memory retrieval. *PloS One*, *7*(11), e48550.

Lu, A., Xu, G., Jin, H., Mo, L., Zhang, J., & Zhang, J. X. (2010). Electrophysiological
evidence for effects of color knowledge in object recognition. *Neuroscience
Letters*, *469*(3), 405–410.

Maris, E., & Oostenveld, R. (2007). Nonparametric statistical testing of EEG-and
MEG-data. *Journal of Neuroscience Methods*, *164*(1), 177–190.

Miyashita, Y. (2004). Cognitive memory: Cellular and network machineries and their
top-down control. *Science*, *306*(5695), 435–440.

Nagai, J., & Yokosawa, K. (2003). What regulates the surface color effect in object
recognition: Color diagnosticity or category. *Technical Report on Attention and
Cognition*, *28*, 1–4.

Naor-Raz, G., Tarr, M. J., & Kersten, D. (2003). Is color an intrinsic property of object
representation? *Perception*, *32*(6), 667–680.

Olkkonen, M., Hansen, T., & Gegenfurtner, K. R. (2008). Color appearance of
familiar objects: Effects of object shape, texture, and illumination changes.
Journal of Vision, *8*(5), 13–13.

Oostenveld, R., Fries, P., Maris, E., & Schoffelen, J.-M. (2011). FieldTrip: Open
source software for advanced analysis of MEG, EEG, and invasive
electrophysiological data. *Computational Intelligence and Neuroscience*,
2011, 1.

Oosterhof, N. N., Connolly, A. C., & Haxby, J. V. (2016). CoSMoMVPA: Multi-modal

multivariate pattern analysis of neuroimaging data in Matlab/GNU Octave.

Frontiers in Neuroinformatics, *10*.

https://www.ncbi.nlm.nih.gov/pmc/articles/PMC4956688/

Papinutto, N., Galantucci, S., Mandelli, M. L., Gesierich, B., Jovicich, J., Caverzasi,

E., Henry, R. G., Seeley, W. W., Miller, B. L., Shapiro, K. A., & Gorno-

Tempini, M. L. (2016). Structural connectivity of the human anterior temporal

lobe: A diffusion magnetic resonance imaging study. *Human Brain Mapping*,

37(6), 2210–2222. https://doi.org/10.1002/hbm.23167

Patterson, K., Nestor, P. J., & Rogers, T. T. (2007). Where do you know what you

know? The representation of semantic knowledge in the human brain. *Nature

Reviews Neuroscience*, *8*(12), 976.

Price, A. R., Bonner, M. F., Peelle, J. E., & Grossman, M. (2017). Neural coding of

fine-grained object knowledge in perirhinal cortex. *BioRxiv*, 194829.

Proverbio, A. M., Burco, F., del Zotto, M., & Zani, A. (2004). Blue piglets?

Electrophysiological evidence for the primacy of shape over color in object

recognition. *Cognitive Brain Research*, *18*(3), 288–300.

https://doi.org/10.1016/j.cogbrainres.2003.10.020

Rosenthal, I., Ratnasingam, S., Haile, T., Eastman, S., Fuller-Deets, J., & Conway,

B. R. (2018). Color statistics of objects, and color tuning of object cortex in

macaque monkey. *Journal of Vision*, *18*(11), 1–1.

Seymour, K., Clifford, C. W. G., Logothetis, N. K., & Bartels, A. (2010). Coding and

Binding of Color and Form in Visual Cortex. *Cerebral Cortex*, *20*(8), 1946–

1954. https://doi.org/10.1093/cercor/bhp265

Seymour, K., Williams, M. A., & Rich, A. N. (2015). The representation of color across the human visual cortex: Distinguishing chromatic signals contributing to object form versus surface color. *Cerebral Cortex*, *26*(5), 1997–2005.

Simmons, W. K., Ramjee, V., Beauchamp, M. S., McRae, K., Martin, A., & Barsalou, L. W. (2007). A common neural substrate for perceiving and knowing about color. *Neuropsychologia*, *45*(12), 2802–2810.

Smith, S. M., & Nichols, T. E. (2009). Threshold-free cluster enhancement: Addressing problems of smoothing, threshold dependence and localisation in cluster inference. *Neuroimage*, *44*(1), 83–98.

Tanaka, J. W., & Presnell, L. M. (1999). Color diagnosticity in object recognition. *Perception & Psychophysics*, *61*(6), 1140–1153. https://doi.org/10.3758/BF03207619

Tanaka, J. W., Weiskopf, D., & Williams, P. (2001). The role of color in high-level vision. *Trends in Cognitive Sciences*, *5*(5), 211–215. https://doi.org/10.1016/S1364-6613(00)01626-0

Teichmann, L., Grootswagers, T., Carlson, T., & Rich, A. N. (2019). Seeing versus knowing: The temporal dynamics of real and implied colour processing in the human brain. *NeuroImage*.

Therriault, D. J., Yaxley, R. H., & Zwaan, R. A. (2009). The role of color diagnosticity in object recognition and representation. *Cognitive Processing*, *10*(4), 335.

Vandenbroucke, A. R., Fahrenfort, J. J., Meuwese, J. D. I., Scholte, H. S., & Lamme, V. A. F. (2014). Prior knowledge about objects determines neural color representation in human visual cortex. *Cerebral Cortex*, *26*(4), 1401–1408.

Wagberg, J. (2007). *OptProp, Matlab toolbox for calculation of color related optical properties*.

Willenbockel, V., Sadr, J., Fiset, D., Horne, G. O., Gosselin, F., & Tanaka, J. W. (2010). Controlling low-level image properties: The SHINE toolbox. *Behavior Research Methods*, *42*(3), 671–684.

Witzel, C., Valkova, H., Hansen, T., & Gegenfurtner, K. R. (2011). Object knowledge modulates colour appearance. *I-Perception*, *2*(1), 13–49.

Zeki, S., & Marini, L. (1998). Three cortical stages of colour processing in the human brain. *Brain: A Journal of Neurology*, *121*(9), 1669–1685.
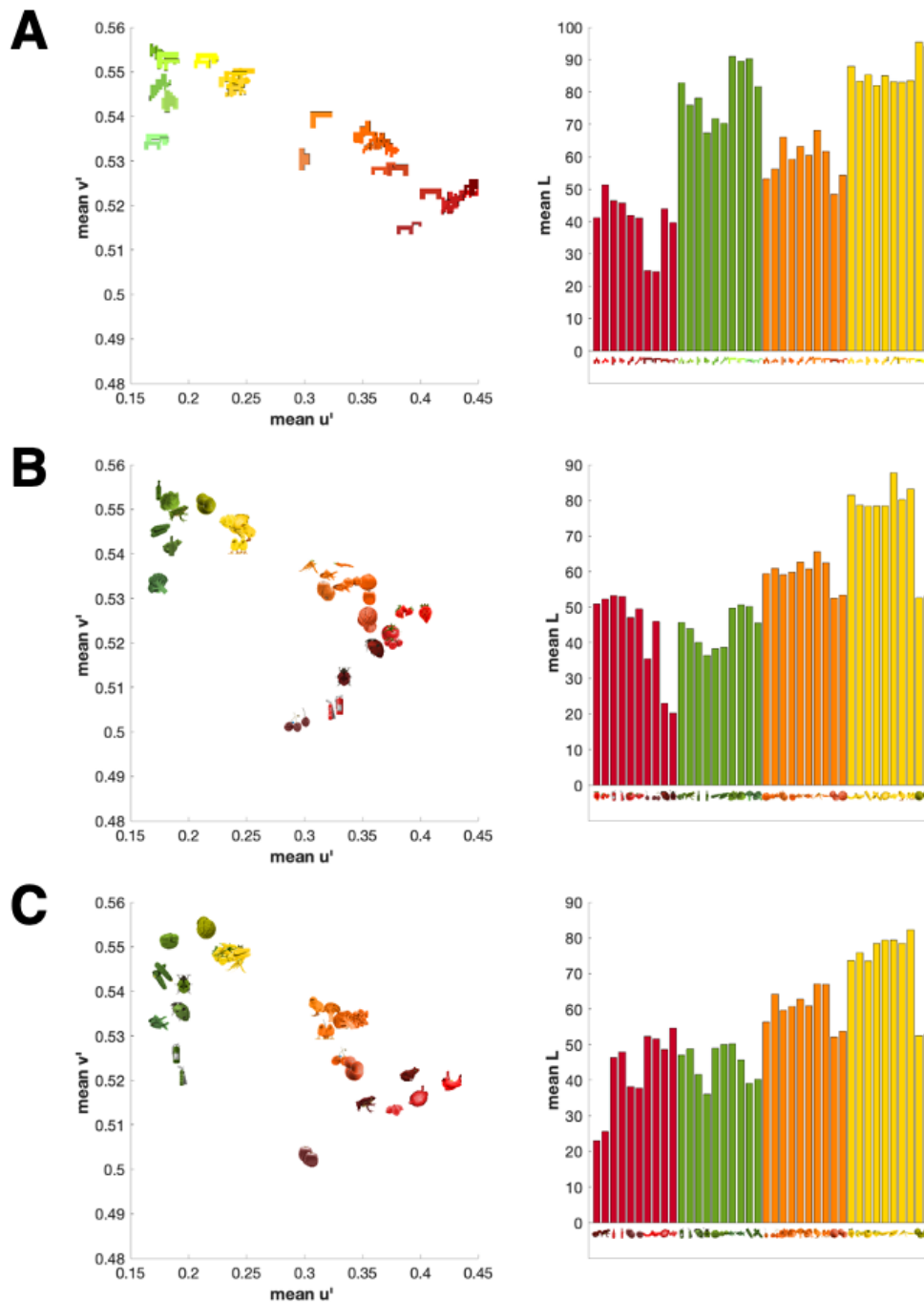
Supplementary Information

Figure SI1: Mean chromaticity coordinates for the 2° observer under D65 illumination as well as the mean lightness of all coloured stimuli used in this experiment. The colours were transformed into CIELUV space using the OptProp toolbox (Wagberg, 2007). Panel (A) shows the chromaticity (u' and v') and lightness (L) for the abstract shapes, panel (B) for the congruently coloured objects, and panel (C) for the incongruently coloured objects.